An Interactive Tool to Model Virtual Abdominal and Cerebral Aneurysms

Rodrigo L. S. Silva, Eduardo Camargo, Pablo Javier Blanco, Márcio Pivello, Rául A. Feijóo
National Laboratory for Scientific Computation
Hemodynamic Modeling Laboratory
Petrópolis, Rio de Janeiro, Brazil
{rodrigo,camargo,pjblanco,pivello,feij}@lncc.br

Abstract: *This paper presents a modeling tool to create hemodynamic pathologies, based on geometrical singularities, such as Aneurysms and Stenoses. An interactive tool that allows the positioning of virtual aneurysms will be explained and some simulation results will be presented. These pathologies can be added based on parameterized geometries or over real arterial geometries, usually obtained via segmentation techniques from medical images. This tool allows modeling cerebral and abdmonimal aneurysms and stenoses interactively.*

1. Introduction

Recently, computational tools to treat cardiovascular diseases are being developed stimulated by the increase of these pathologies. The complexity of these surgical interventions is notably growing in the last years due the fast advances in modern medicine. Some cardiovascular diseases, such as arterioscleroses and cerebral aneurysms, are reported to depend on hemodynamic factors, particularly on the characteristics of the wall shear stress induced by blood flow [1]. With the purpose of joining tools to aid the treatment of these diseases a computational environment called HeMoLab was created [6]. HeMoLab is a computer system that allows the creation of patient-oriented models of the human cardiovascular system and also the numerical simulation within a unified framework.

To allow a better study of the cardiovascular diseases, it is necessary to model a 3D representation of the human cardiovascular system (HCS). This modeling aims to study with a high level of detail the hemodynamic features of the blood flow and how those features are modified when, for instance, a surgical planning is devised over such system. Patient-specific data can be used to represente in details any part of the arterial network by using information like medical images of the arterial district of interest. Particular cases, like the presence of geometric singularities (aneurysm, stenoses, bifurcations and so on) can be simulated in order to study local changes in the blood flow structure and used to retrieve a more complete quantitative information.

A complete simulation is composed by the reconstruction of the geometrical data through medical imaging systems (Magnetic Resonance Imaging and Computed Tomography), determination of boundary conditions and mechanical properties of the blood and arterial walls of the selected area and finally the computation of an approximate solution of the problem. Due to the high complexity of the simulation of a full 3D HCS, just the arterial district of interest is represented in 3D. The rest of the HCS is represented using a simplified 1D model [3].

This paper presents an interactive system to create and simulate virtual abdominal aneurysms over parameterized geometrical structures and patient-based arteries. This interactivity allows the user to simulate aneurysms with different sizes and different positions. Numerical results can be graphically presented using visualization techniques such as stream-lines, stream-tubes, warping techniques for the velocity field, etc.

The tool developed in this paper was integrated into the HeMoLab system that, in turn, is supported by the ParaView architecture [11]. ParaView is a point-and-click 3D scientific visualization system that allows for most of the common visualization techniques (isocontouring, volume rendering) on structured and unstructured grids. Its implementation uses distributed memory parallelism, and is focused on visual data analysis of large scientific datasets. It is an open-source, multi-platform visualization application, and supports distributed computation models to process large datasets. It has an open, flexible, and intuitive user interface and an extensible architecture based on the Visualization Toolkit (VTK) [19].

The remainder of this work is organized as follows: Section 2 presents a brief survey of some works related to computer modelling of the cardiovascular system. In Section 3 the algorithm for the generation of aneurysms and stenoses is detailed, whereas mathematical modelling and numerical approximation of the physical phenomena involved are described in Sections 4. Results obtained after simulating the flow inside a patient-specific artery modified by the tools presented here are shown in Section 5, and some concluding remarks are listed in Section 6.

2. Related Works

Some work oriented to the treatment, visualization, simulation and diagnosis of stenoses and aneurysms can be viewed in [9, 10, 12, 14]. A training system developed with medical purposes was proposed in [7]. The system enables the instructor to generate specific cases for analysis, allowing to gain insight not only in the basic feature of searching and stenosis evaluation processes, but also about the importance of the correct viewpoint of acquisition within the environment.

In [8] the authors propose an algorithm that decomposes the patterns of 3D unsteady blood flow into behavioral components to reduce the visual complexity while retaining the structure and information of the original data. The key point of the algorithm is to enable the visualization of large simulated data sets avoiding visual clutter and ambiguity.

Previous versions of the system proposed in this article were able to model cerebral aneurysms and stenoses as presented in [13]. Also some preliminary numerical simulation results were presented. This paper differs from these works approaches by extending the usability of the system presented in [13] to model not only cerebral aneurysms but also abdominal. These extensions were accomplished by the generalization of the algorithms that allows the addiction of spherical meshes over synthetic and real arterial districts. This paper also presents some comparisons between the simulation of real and synthetics aneurysms.

3. Modeling Abdominal Aneurysms

The main feature of the tool presented in this paper is the ability to easily merge two meshes so as to create new geometries maintaining the correct topology. Basically one or more sphere meshes are merged over synthetic and real arterial districts.

Creating abdominal aneurysms require the following steps:

- set the sphere widget in the right position;
- clip the main surface with the widget;
- find boundary triangles on the clipped area;
- find the intersection between the clipped surface and the sphere widget;
- merge the two (or more) surfaces discarding the unused triangles on the sphere and the ones over the original geometry;

The system provides a sphere widget to be added on a given region to create an aneurysm. The user can change the position of the widget by clicking over it in the render interface or change that position numerically in the parameter interface. The radius and the resolution of the widget can also be changed (Figure 1).

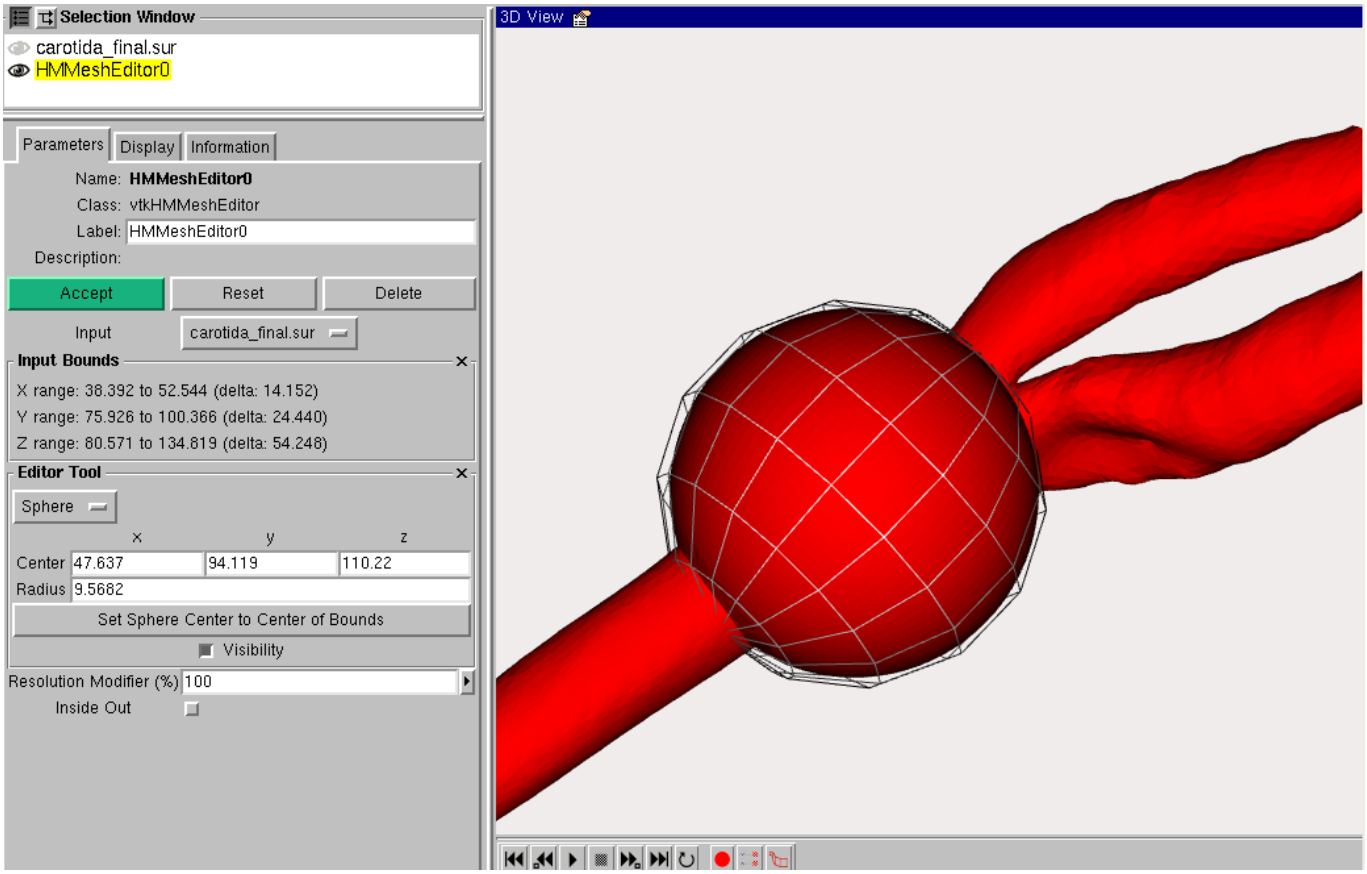

Figure 1. System interface. The sphere widget is represented in wireframe mode.

3.1 Merging surfaces

One of the major problems of creating the pathologies mentioned above was to merge different meshes while preserving the consistency of the topology, connectivity and point sharing. To address these issues, the resolution of the spherical widget and the resolution of the main mesh should be as similar as possible. In this situation, joining the two meshes is easier, because the number of points to be joined in the clipped surface and the sphere is similar. The initial resolution of the sphere widget is automatically selected based on the average size of the input triangle mesh. Although, the user can change this resolution to refine the sphere or make it more rough. Figure 2 shows several resolution values applied to the same widget to illustrate this feature.

Depending on the position of the widget, the system will produce an aneurysm or a stenoses. Also, when the widget cuts the main mesh in two pieces, abdominal aneurysms can be created. If the widget do not split the main mesh, cerebral aneurysms can be modeled. Figures 3.a, 3.b e 3.c presents examples of stenoses, cerebral aneurysms and abdominal aneurysms.

Figure 4 illustrate the use of the tool to model several sizes of virtual abdominal aneurysms. An user can change the size of the sphere widget by right-clicking on the render interface or by changing the radius entry on the parameter interface.

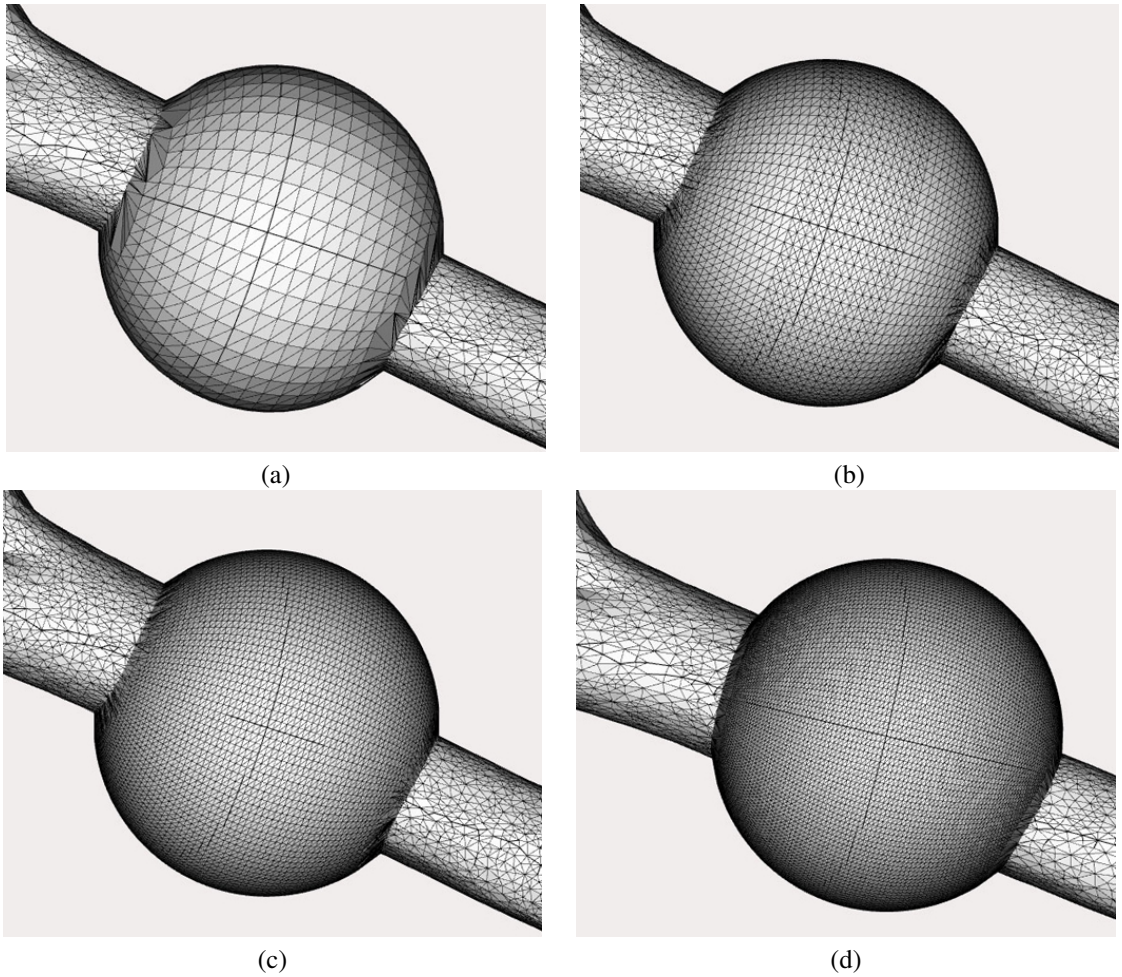

Figure 2. Abdominal aneurysms with different resolutions. The resolution modifier was set to (a) 50%, (b) 100%, (c) 150% and (d) 220%.

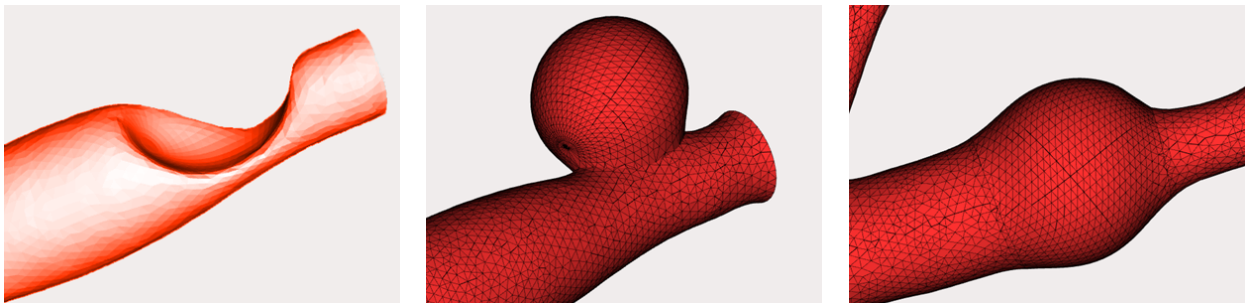

Figure 3. Example of (a) Stenoses, (b) Cerebral aneurysm and (c) abdominal aneurysms.

4 Mathematical Model of the coupled 3D – 1D blood flow simulation

Blood flow simulation is performed with a coupled 3D – 1D model of the arterial system, which consists in embedding a 3D model of an artery in a simplified 1D model of the arterial system. Inlets and outlets of the 3D model are coupled with their respective counterparts in the 1D model, such that no 3D boundary condition is necessary. The main advantage of using

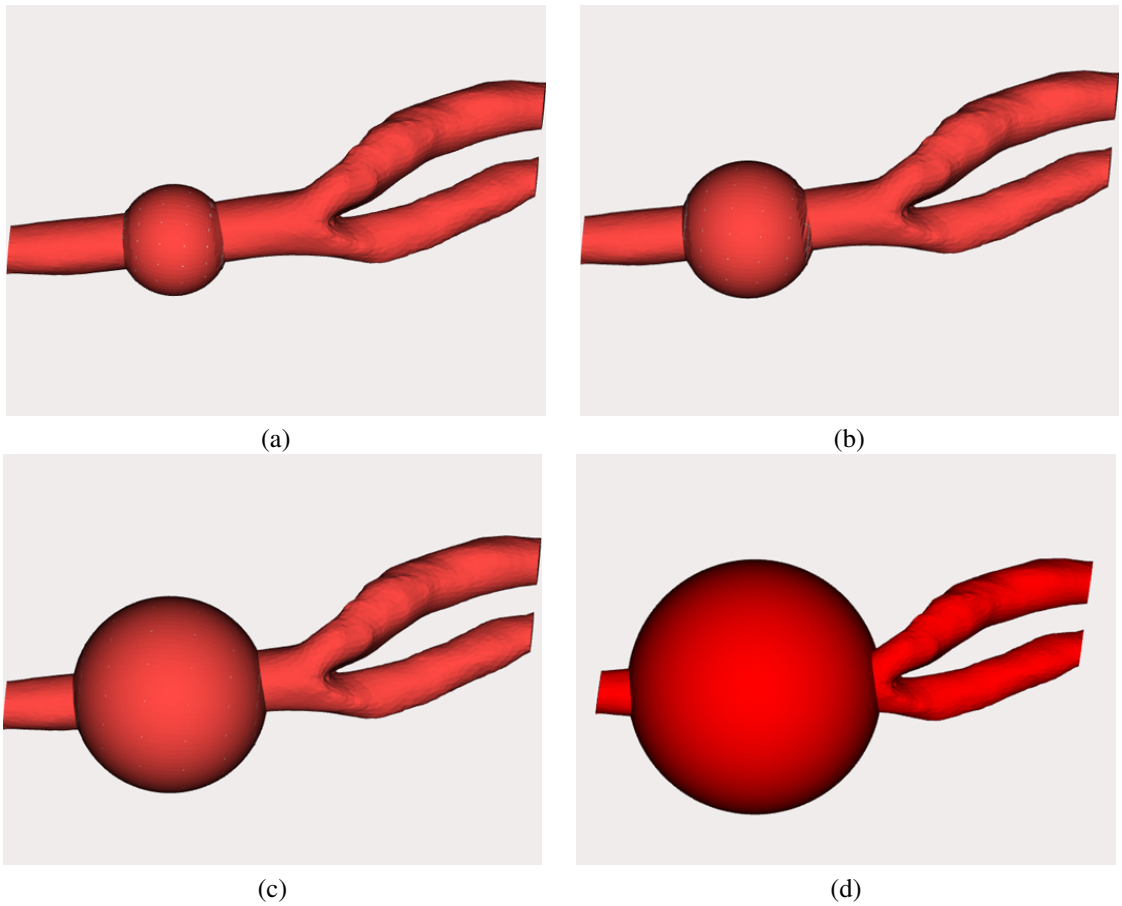

(a) (b)

(c) (d)

Figure 4. Abdominal aneurysms with different sizes.

3D–1D coupled models is that they behave as a unique system, avoiding the need for measurements that would be required when employing standalone 3D models. The boundary conditions over the inlets-outlets of the 3D region are accounted for the own solution of the entire problem. In other words, it can be understood in the following way: the 1D model feeds the 3D model with certain conditions and vice-versa. On the other hand, the boundary conditions needed are the heart inflow boundary condition that represents the heart ejection and the Windkessel terminals, which are used to simulate the peripheral beds not included in the model. Therefore, once the 1D model is calibrated and validated, any artery which is present in the model may be replaced by a detailed 3D counterpart that is able to yield richer qualitative and quantitative results about the flow patterns in that region. This is particularly useful when studying pathologies such as aneurysm, stenoses, etc. which are phenomena based on local factors.

The governing equations were derived based on a variational formulation for the coupling of kinematically incompatible models, in this case 3D-1D flow models in compliant vessels [3]. The associated Euler equations for a Newtonian fluid when coupling a 1D domain Ω_{1D} with a 3D region Ω_{3D} through a coupling interface Γ_c, and considering the ALE

(Arbitrary Lagrangian Eulerian) formulation over Ω_{3D}, are the following:

$$\rho A\frac{\partial \bar{u}}{\partial t} + \rho A\bar{u}\frac{\partial \bar{u}}{\partial z} = -A\frac{\partial \bar{p}}{\partial z} - 8\pi\mu\bar{u} + f^z \quad \text{in } \Omega_{1D}\times(0,T) \tag{1}$$

$$\rho\frac{\partial \mathbf{u}}{\partial t}\bigg|_{\mathbf{Y}} + \rho\nabla\mathbf{u}\,(\mathbf{u}-\mathbf{w}) = -\nabla p + \mu\Delta\mathbf{u} + \mathbf{f} \quad \text{in } \Omega_{3D}\times(0,T) \tag{2}$$

$$\frac{\partial A}{\partial t} + \frac{\partial\,(A\bar{u})}{\partial z} = 0 \quad \text{in } \Omega_{1D}\times(0,T) \tag{3}$$

$$\nabla\cdot\mathbf{u} = 0 \quad \text{in } \Omega_{3D}\times(0,T) \tag{4}$$

$$(-p\mathbf{I} + 2\mu\boldsymbol{\varepsilon}(\mathbf{u}))\,\mathbf{n}_1 = -\bar{p}\mathbf{n}_1 \quad \text{on } \Gamma_c\times(0,T) \tag{5}$$

$$A_c\bar{u} = \int_{\Gamma_c}\mathbf{u}\cdot\mathbf{n}_1\,d\Gamma \quad \text{on } \Gamma_c\times(0,T) \tag{6}$$

Where $\mathbf{n}_1$ is the unit outward normal to domain Ω_{1D} over the coupling interface Γ_c. In equations 1 and 3, which represent the 1D model, $\bar{u}$, $\bar{p}$ are the mean velocity and pressure values, ρ is the blood density, μ is the dynamic viscosity, A denotes the cross sectional area, $Q = A\bar{u}$ is the flow rate and z is the axial coordinate. Equations 2 and 4 represent the 3D model, $\mathbf{u}$ is the blood velocity, $\mathbf{w}$ is the domain velocity of change consistent with the ALE framework, while p is the blood pressure. Equation 5 stands for the continuity of the traction vector at Γ_c (the coupling interface between the 3D and 1D models), while expression 6 is the counterpart of the mass conservation.

The wall movement is modelled according to the independent ring model [4], and its equations are stated bellow:

$$\bar{p} = \bar{p}_0 + \frac{E\pi R_0 h_0}{A}\left(\sqrt{\frac{A}{A_0}} - 1\right) + \\ + \frac{k\pi R_0 h_0}{A}\frac{1}{2\sqrt{A_0 A}}\frac{\mathrm{d}A}{\mathrm{d}t} \text{ in } \Omega_{1D}\times(0,T) \tag{7}$$

$$p = p_0 + \frac{Eh}{R_0^2}\zeta + \frac{kh}{R_0^2}\frac{\mathrm{d}\zeta}{\mathrm{d}t} \quad \text{in } \Gamma_w\times(0,T) \tag{8}$$

This is a rather simplified model of the structural behavior of the arterial wall, but serves to take into account the arterial compliance. The deformation of the domain Ω_{3D} is accounted for through a Laplacian problem, as stated bellow:

$$\nabla^2\mathbf{d} = 0 \qquad \text{in} \qquad \Omega_{3D}\times(0,T) \tag{9}$$

Since it is a small amplitude movement, no remeshing is performed. Instead, equation 9 is used in order to extend the wall movement to the interior of Ω_{3D}, and $\mathbf{d}|_{\Gamma_w} = \zeta\mathbf{n}$ is the wall displacement, where ζ is the scalar field that denotes the displacement of the wall in the normal direction, given by $\mathbf{n}$, that is obtained from equation 8. Finally, it is $\mathbf{w} = \frac{\partial\mathbf{d}}{\partial t}$. Refer to [3] for a further theoretical account about the coupling of 3D-1D blood flow models.

5 Results

In order to show the usability of the tool described above, we present the results of the flow simulation inside a segment of the abdominal aorta in two situations: (i): when an aneurysm was added to it with the tool described before and (ii) when the

healthy artery was used, for comparison purposes. Another case is presented, in which the flow inside an arterial segment of the pericallosal artery with a natural aneurism is compared to the flow when an artificial aneurism is included in the same artery.

Figure 5 shows a comparison between a segment of a healthy abdominal aorta (Figure 5.a), and the same segment after the insertion of an aneurism with the tool described in this work. In Figure 5.c it is possible to see both geometries overlayed.

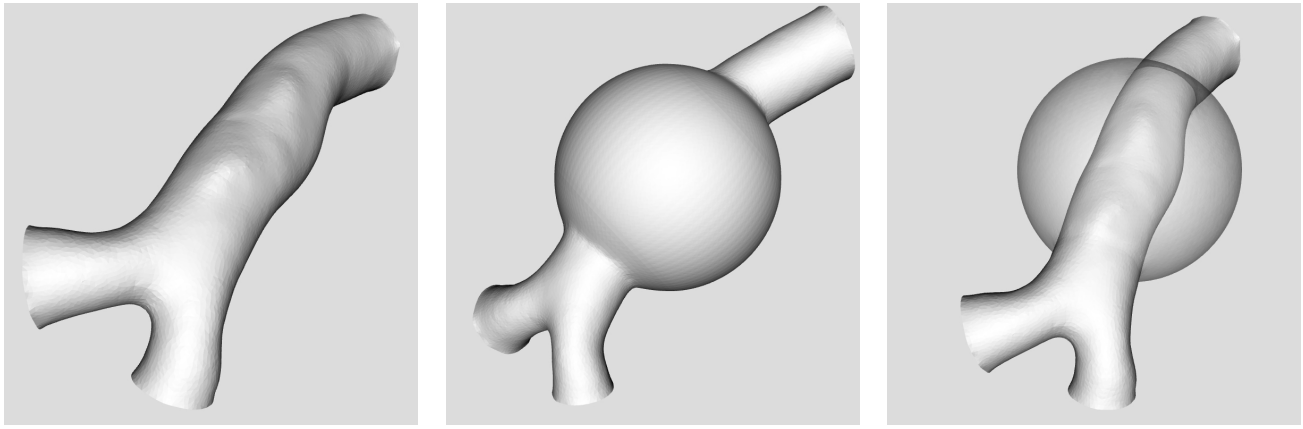

(a) (b) (c)

Figure 5. A segment of the abdominal aorta without aneurism (a), with an aneurism generated artificially (b) and both cases overlayed (c).

Figure 6 shows some characteristics of the flow in the healthy aorta segment at some time instant in the systolic phase of a heart beat. Notice that the streamlines (Figure 6.a), which represent lines tangent to the velocity field at a given time, show a laminar flow, without recirculation. This is confirmed by Figure 6.b, which shows the profile of the modulus of the velocity at some planes. The overlaying of both can be seen in Figure 6.c.

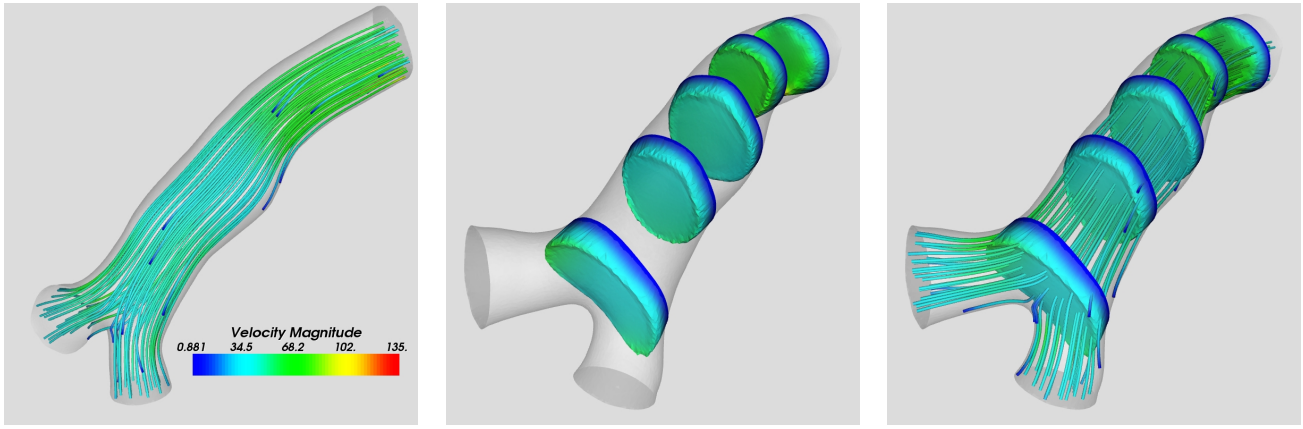

(a) (b) (c)

Figure 6. Characteristics of the flow in the healthy aorta: Streamlines (a), velocity profiles (b) and both overlayed (c).

Comparing Figure 6 and Figure 7 it is possible to see the differences caused by the presence of the aneurism. Notice that, after entering that region, there is an important variation in the velocity field, due to both a change in the sectional area

and an increase in the geometric complexity of the domain. These figures also show results during the systolic phase.

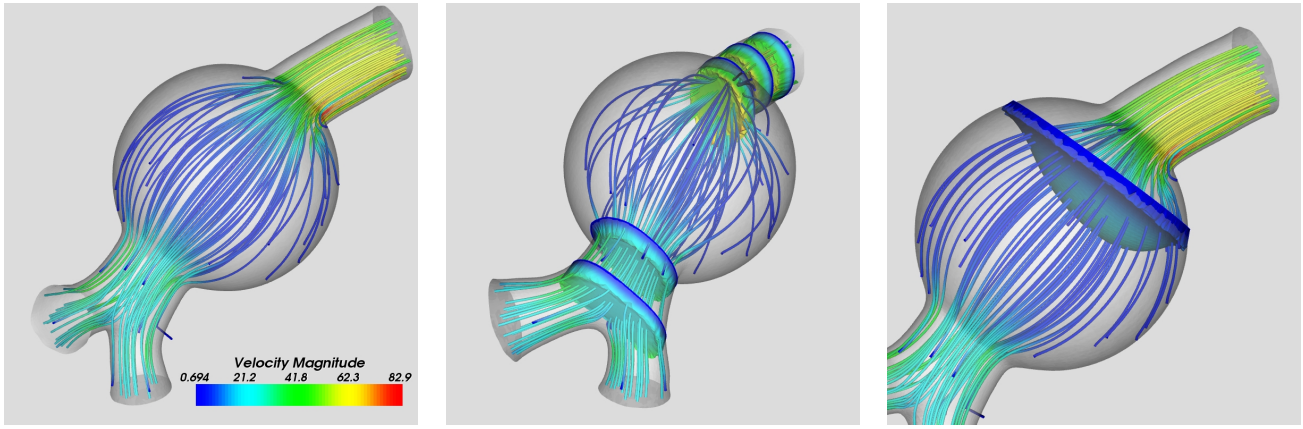

(a) (b) (c)

Figure 7. Details of the flow after inserting of the aneurism. Streamlines (a), streamlines and modulus of the velocity profile and a zoom in the region of the aneurism (c).

Figure 8 shows two segments of the pericallosal artery belonging to the same individual: namely a natural aneurism (Figure 8.a), an artificial aneurism (Figure 8.b) and a comparison between both (Figure 8.c). The natural aneurism is located in the right pericallosal artery and the artificial one is on the left artery. The goal here is to assess differences in the flow inside the aneurism in both cases. These comparisons could justify the uses of this class of tools to represent geometric singularities.

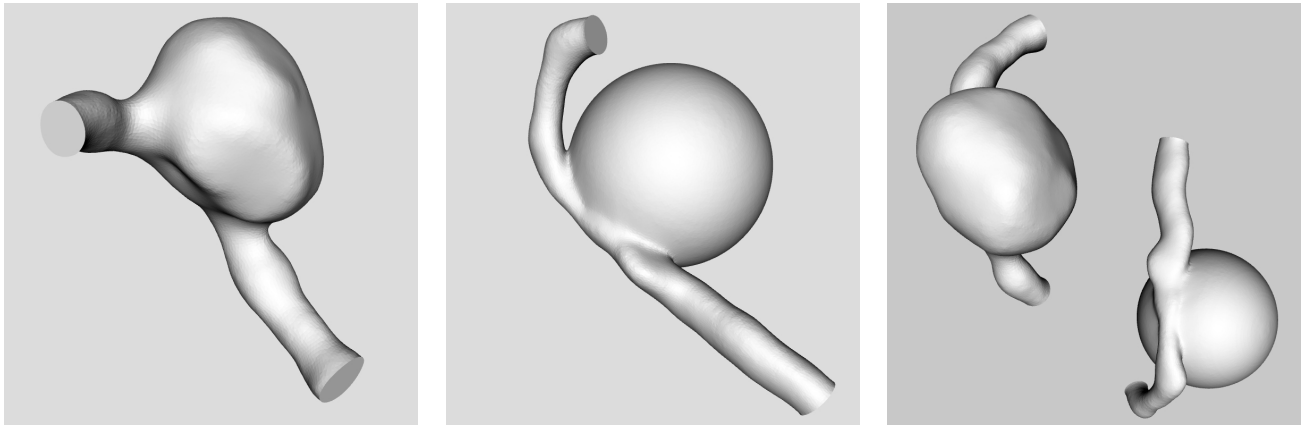

(a) (b) (c)

Figure 8. Comparison between a natural aneurism in the pericallosal artery and an artificial aneurism generated in the same artery.

Figure 9 shows some preliminary results of the flow in the segment with the natural aneurism. It is easy to see that both velocity profiles and streamlines are highly complex inside the aneurism.

Figure 10 shows the flow in the arterial segment with an artificial aneurism. Some characteristics present in the natural aneurism may be identified here, such like the decrease of the velocity and the greater complexity of the flow inside the aneurism. Both results, from Figure 9 and Figure 10, correspond to the systolic phase of the heart beat. We expect the results in the dyastolic phase to present more significant differences and similitudes.

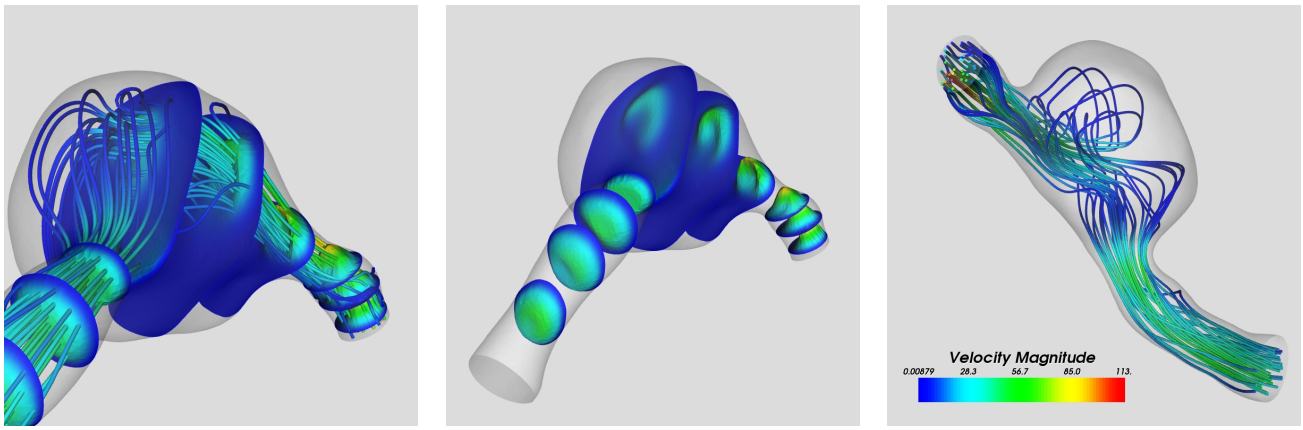

(a) (b) (c)

Figure 9. Details of the flow in the arterial segment with a natural aneurism: streamlines (a), velocity profile (b) and a zoom inside the aneurism, with streamlines and velocity profiles overlayed.

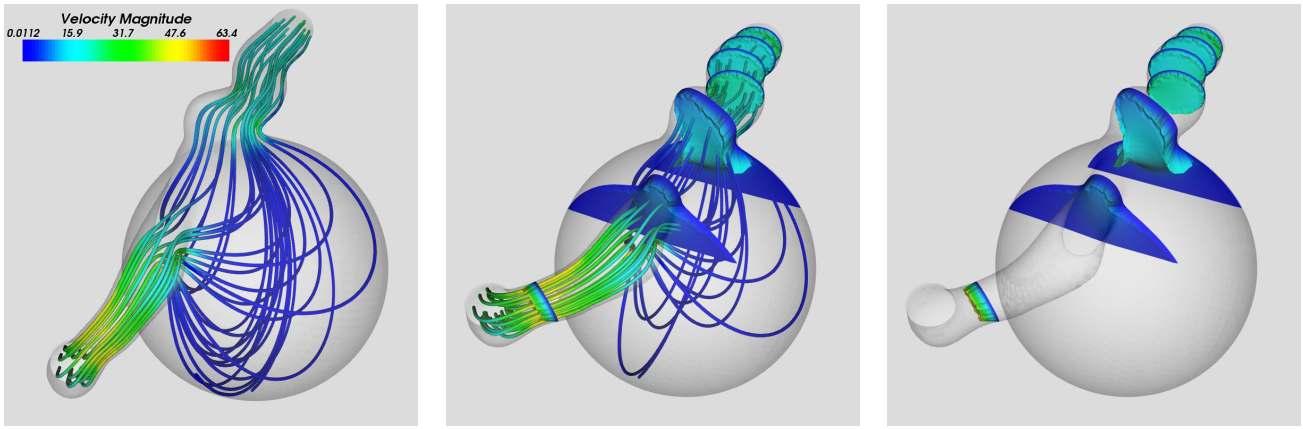

(a) (b) (c)

Figure 10. Details of the flow in the arterial segment with an artificial aneurism: streamlines (a), velocity profile (b) and streamlines and velocity profiles overlayed.

6. Conclusions

This work presents a tool to model and simulate pathologies arising in cardiovascular modeling such as Aneurysms and Stenoses. The geometrical models can be interactively constructed through the manipulation of spherical widgets over a given geometry representing an arterial district of interest.

After the reconstruction of the geometrical singularity that represents the pathology, the system allows in a straightforward way the computation of an approximate solution through the numerical simulation. The numerical results have been then analyzed using several visualization techniques such as stream lines, isosurfaces, arbitrary slices, warping techniques, etc. From the obtained numerical evidences it can be said that this kind of tool permits the characterization, through diverse numerical indicators, of the altered physical phenomena that occur when different anomalies are present in the cardiovascular system.

References

[1] A.M. Malek, S.L. Alper, and S. Izumo. Hemodynamic shear stress and its role in atherosclerosis. *JAMA*, 282(21):2035–2042, December 1999.

[2] D. Arnold, F. Brezzi, and M. Fortin. A stable finite element for the stokes equations. *Calcolo*, 21(1), 1984.

[3] P. Blanco, R. Feijóo, and S. Urquiza. A unified variational approach for coupling 3D–1D models and its blood flow applications. *Comp. Meth. Appl. Mech. Engrg.*, 196:4391–4410, 2007.

[4] Y. Kivity and R. Collins. Nonlinear fluid–shell interactions: application to blood flow in large arteries. *Int. Sym. Discrete Meth. Engrg.*, pages 476–488, 1974.

[5] I. Larrabide. *Processamento de imagens via derivada topológica e suas aplicações na modelagem e simulação do sistema cardiovascular humano*. PhD thesis, National Laboratory for Scientific Computation, 2007.

[6] I. Larrabide and R. Feijóo. HeMoLab: Laboratório de Modelagem em Hemodinâmica. Technical Report 13/2006, National Laboratory for Scientific Computing, 2006.

[7] I. Lebar Bajec, P. Trunk, D. Oseli, and N. Zimic. Virtual coronary cineangiography. *Computers in Biology and Medicine*, 33(3):293–302, 2003.

[8] D. Lee, D. J. Valentino, G. R. Duckwiler, and W. J. Karplus. Simulation and virtual-reality visualization of blood hemodynamics: the virtual aneurysm. In *Proceedings of SPIE*, volume 4319, pages 465–470, May 2001.

[9] M.R. Harreld. Modeling, Simulation and VR Visualization of Brain Aneurysm Blood Flow. Technical Report 960018, UCLA Computer Science Department, 1996.

[10] M. Oshima. A New Approach to Cerebral Hemodynamics: Patient-Specific Modeling and Numerical Simulation of Blood Flow and Arterial Wall Interaction. *Bulletin for The International Association for Computational Mechanics*, 14:4–9, 2004.

[11] ParaView. http://www.paraview,org.

[12] Y. Sato, T. Araki, and M. Hanayama. A Viewpoint Determination System for Stenosis Diagnosis and Quantification in Coronary Angiographic Image Acquisition. In *IEEE Transaction Medical Imaging*, volume 17, pages 121–137, 1998.

[13] R. Silva, P. Blanco, M. Pivello, and R. Feijóo. Virtual modeling and numerical simulation of aneurysms and stenoses. *X Symposium on Virtual and Augmented Reality*, 2008.

[14] N. Stergiopulos, D.F. Young, and T.R. Rogge. Computer Simulation of Arterial Flow with Applications to Arterial and Aortic Stenoses. In *Journal of Biomechanics*, volume 25, pages 1477–1488, 1992.

[15] T.J.R. Hughes, L.P. Franca, and M. Mallet. A new finite element formulation for computational fluid dynamics: Vi. convergence analysis of the generalized supg formulation for linear time-dependent multi-dimensional advective-diffusive systems. *Comput. Methods Appl. Mech. Eng.*, 63(1):97–112, 1987.

[16] S. Urquiza, P. Blanco, M. Vénere, and R. Feijóo. Multidimensional modeling for the carotid blood flow. *Comput. Meth. Appl. Mech. Engrg.*, 195:4002–4017, 2006.

[17] M. Vénere. Procedimientos para la generación de mallas tridimensionales de elementos finitos. *Revista internacional de Métodos Numéricos para cálculo y diseño en ingenieria*, 12:3–16, 1996.

[18] M. Vénere. Optimización de la calidad de mallas de elementos finitos mediante cambios localizados de topologia. *Revista internacional de Métodos Numéricos para cálculo y diseño en ingenieria*, 13:3–13, 1997.

[19] VTK - Visualization Toolkit. http://www.vtk.org.